View metadata, citation and similar papers at core.ac.uk

brought to you by CORE

provided by Elsevier - Publisher Connector

Size Effects in Ion-Neutral Complex-Mediated Alkane Eliminations from Ionized Aliphatic Ethers

David J. McAdoo and Charles E. Hudson
Marine Biomedical Institute, University of Texas Medical Branch, Galveston, Texas, USA

John C. Traeger
Chemistry Department, LaTrobe University, Bundoora, Victoria, Australia

Andrew Grose and Lawrence L. Griffin
Department of Marine Sciences, Texas A&M University at Galveston, Galveston, Texas, USA

The effects of the size of the ionic and neutral partners on ion-neutral complex-mediated alkane eliminations from ionized aliphatic ethers were determined by obtaining metastable decomposition spectra and photoionization ionization efficiency curves. Increasing the size of the ionic partner decreases the competitiveness of alkane elimination with alkyl loss. This is attributed to decreasing attraction between the partners with increasing distance between the neutral partner and the center of charge in the associated ion. Increasing the size of the neutral partner lowers the threshold for alkane elimination relative to that for simple dissociation when the first threshold is above ΔH_f(products). This is attributed to increasing attraction between the partners with increasing polarizability of the radical in the complex. Adding a CH_2 to the radical in a complex seems to increase the attraction between the partners by about 24 kJ mol^{-1}. *(J Am Soc Mass Spectrom 1991, 2, 261–269)*

Alkane eliminations from ionized ketones in the gas phase seem to become less important with increasing size of the ionic product and more important with increasing size of the neutral fragment [1]. These eliminations involve hydrogen transfers in intermediate ion-neutral complexes [1,2], reactions which depend strongly on the energy content of the fragmenting ion [1,3]. Size effects on this dependence are of interest because they illuminate dynamics of ion-molecule reactions at very low energies.

The partners in intermediate complexes are held in association by ion-dipole and ion-induced dipole attractions. When the neutral partner is nonpolar and the partners are far enough apart that valence forces are not important, the binding energy between the partners is approximated by the formula

$$E = \alpha q^2/2r^4 \qquad (1)$$

where α is the polarizability of the neutral, q is the charge on the ion, and r is the distance between the center of charge and the neutral. Increasing the size of the ion in the complex should increase r, and therefore decrease the attraction between the partners. This would in turn diminish the competitiveness of internal ion-molecule reactions with associated simple dissociations. On the other hand, the polarizability of alkyl radicals increases with increasing radical size, and therefore so should forces of attraction between them and nearby ions.

The effects of the size of the two types of partners (charged and neutral) were not well separated in our studies of ionized ketones [1]. Therefore, we here investigate size effects more systematically by varying the sizes of the partners in intermediate complexes in decompositions of ionized ethers (Scheme I). Ion-neutral complexes are depicted by placing the partners within brackets.

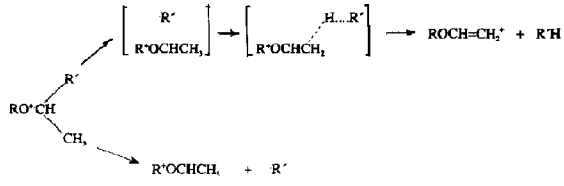

Scheme I

Address reprint requests to David J. McAdoo, Marine Biomedical Institute, University of Texas Medical Branch, 200 University Boulevard, Galveston, TX 77550.

© 1991 American Society for Mass Spectrometry
1044-0305/91/$3.50

Received November 12, 1990
Accepted January 29, 1991

Results and Discussion

Size effects, potential energy surfaces, and photoionization ionization efficiency curves. One determinant of the importance of alkane elimination relative to alkyl loss is the difference between the thresholds for the two processes. We obtained these differences by determining photoionization appearance energies. The difference AE(−R′) − AE(−R′H) is hereafter referred to as ΔAE. A substantial fraction of a complex-mediated alkane elimination often occurs below the threshold for alkyl loss [1,2c,3], so increasing ΔAE should enhance alkane loss. Size effects will affect the contours of the potential surface in the regions on which R′H eliminations occur, and hence ΔAE.

To understand what determines ΔAE, it is useful to assume that there are two local energy maxima in the pathway to alkane elimination, one at the transition state for reorientation of the partners to the H-transfer configuration, and one during hydrogen transfer. However, the first transition state may be more an entropic minimum than an energy maximum [4]. A previous discussion of isotope effects suggests that either transition state may be rate determining [2c]. Barriers to H-transfer may place the onset energy for R′H elimination above the energy required to form the complex $[R^+OCHCH_3\ R']$ and above $\Delta H_f(ROCH = CH_2^+) + \Delta H_f(R'H)$. The onset for R′H elimination would then be the energy at which tunneling through the barrier to H-transfer becomes appreciable (Figure 1, top traces) [5]. $[R^+OCHCH_3\ R']$ and $[R^+OCH = CH_2^{+\cdot}\ R'H]$ may both be accessible below ΔH_f of the products of alkane elimination (Figure 1, middle traces). ΔAE will then be equal to the difference between the heats of formation of the products of the two decompositions. Finally, the threshold for forming $[R^+OCHCH_3\ R']$ can be above ΔH_f(−R′H products) (Figure 1, bottom traces). When this occurs, ΔAE might be estimable by eq 1.

Photoionization ionization efficiency (PIE) curves for losses of R′ and R′H (Figures 2–4) provide ΔAE and other information on competition between the two processes. Appearance energies derived from such measurements are given in Table 1. The number of ions formed at an ion energy content corresponding to a value on the abscissa minus the ionization energy of the parent molecule is proportional to the slope of the corresponding PIE curve at that point [6]. That is, at energies at which a curve is rising steeply, the corresponding process is substantial, and at energies where the curve is horizontal, no product containing the full energy $h\nu$ − IE is formed. As with previously studied alkane eliminations [1,3], all of the curves for alkane eliminations reach plateaus not too far above the onset of R′ loss, confirming again that complex-mediated alkane eliminations are largely confined to a narrow energy range near threshold. The decompositions of metastable ions provide reaction patterns very close to threshold.

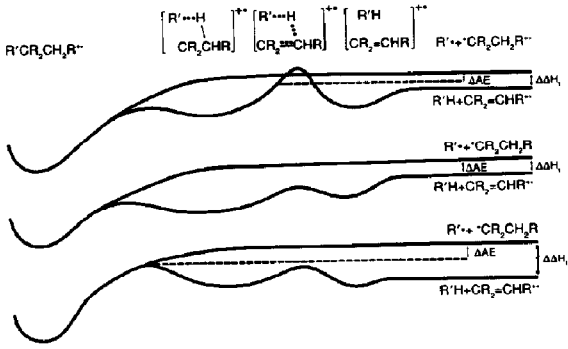

Figure 1. Sections through the potential energy surfaces for complex-mediated dissociations. The species present in each region of the curve is depicted above that section. R′ represents an alkyl radical, and R may be H, an alkyl radical, or some other moiety. The upper pair of traces represents a case in which the barrier to H-transfer is higher than the threshold for simple dissociation. In this case, the threshold for alkane elimination may be set by tunneling through this barrier [5]. In the middle pair of traces complex formation and H-transfer occur below the thermochemical threshold for alkane elimination, so ΔAE and $\Delta\Delta H_f$ will be identical. In the bottom pair of traces the transition state for complex formation is above that for H-transfer, so the threshold for alkane elimination is set by the threshold for $[R'\ CR_2CH_2R]^{+\cdot}$ formation. In this case, ΔAE will be substantially smaller than $\Delta\Delta H_f$.

A problem in the data is that ΔAE is sometimes larger than the differences between published (see Appendix) heats of formation ($\Delta\Delta H_f$) for the products (Table 2), reflecting inconsistency between published and presently derived heats of formation of the vinyl ether products (see below). The following discussion will assume that the AE measurements reflect the threshold differences, as these measurements were made under the same conditions.

Product ion identity. To establish the validity of Scheme I, we confirmed the identity of the products of alkane elimination from the ionized ethers. Methane elimination from ionized isopropyl methyl ether forms the methyl vinyl ether ion [3a,7]. The collisionally activated dissociation (CAD) spectrum of the product of ethane elimination from the metastable *sec*-butyl methyl ether ion matches closely that of ionized methyl vinyl ether (Table 3) and differs significantly from published CAD spectra of other $C_3H_6O^{+\cdot}$ ions [8]. Ethane eliminated from the ionized *sec*-butyl methyl ether ion is composed of the ethyl and a methyl H from the *sec*-butyl group [9]. These results are consistent with ethane elimination from ionized *sec*-butyl methyl ether forming $CH_3OCH = CH_2^{+\cdot}$, as depicted in Scheme I. Similarly, the CAD spectra of the products of metastable RH elimination from a series of ethyl *sec*-alkyl ethers match well the CAD spectrum of $CH_3CH_2OCH = CH_2^{+\cdot}$ (Table 3). The CAD spectra of most $C_4H_8O^{+\cdot}$ ions [10] contain large peaks at m/z 57, in contrast to the low abundance of

Table 1. Photoionization appearance energies and derived thermochemistry for ionized ethers

Ether	IE	AE(−R)	AE(−RH)	$\Delta H_{cor}(-R)^a$	$\Delta H_{cor}(-RH)^a$	$\Delta H_f(-R)^b$	$\Delta H_f(-RH)^b$
$CH_3OCH(CH_3)_2$	917	937	935	20	18	561	776
$CH_3OCH(CH_3)C_2H_5$	898	927	901	22	20	559	733
$CH_3OCH(CH_3)C_3H_7$	896[c]	924	≤ 896[d]	24	22	560	≤ 730
$CH_3OCH(CH_3)C_4H_9$	895	928	≤ 895[d]	26	24	567	≤ 731
$CH_3CH_2OCH(CH_3)_2$	898	900	—[e]	22	20	491	—
$CH_3CH_2OCH(CH_3)C_2H_5$	891	898	895	24	22	498	694
$CH_3CH_2OCH(CH_3)C_3H_7$	886	916	894	26	24	519	695
$CH_3CH_2OCH(CH_3)C_4H_9$	885	916	895	28	26	522	698
$CH_3CH_2CH_2OCH(CH_3)C_2H_5$	887	900	893	26	24	480	672
$(CH_3)_2CHOCH(CH_3)C_2H_5$	871	891	881	28	26	462	652
$[CH_3CH_2CH(CH_3)]_2O$	870	880	875	30	8	432	627

All values are kJ mol^{-1}.
Related published heats of formation are given in the Appendix.
[a]ΔH_{corr} is a statistical mechanical correction factor for thermal energy content [15a]; most ΔH_{cor} values were estimated based on computed reference values and normal increments per added CH_2 group.
[b]The procedure whereby heats of formation of product ions were obtained from the AE measurements is described under Experimental.
[c]Measured onset uncertain.
[d]Values are upper limits because AE equals the ionization potential of the precursor compound.
[e]Ion abundance too low to permit AE measurement.

that species in the $C_4H_8O^{+\cdot}$ spectra obtained in the present study. Thus, the alkane eliminations we examine here appear to form vinyl ether ions, in accord with Scheme I.

Effect of the size of the ionic partner on alkane elimination. The size of the ion in the complex was increased by increasing the size of R in isopropyl and *sec*-butyl ether ions. The importance of methane loss from metastable isopropyl ether ions decreases as the size of the ionic partner increases (Table 4). The patterns vary from negligible methyl loss from ionized isopropyl methyl ether to negligible methane loss from ionized *n*-butyl isopropyl ether, a variation greater than 10^4 in the ratio of the abundances of the two products. Methane elimination from metastable *tert*-butyl ether ions also diminishes rapidly in importance with increasing size of the ionic partner (Table 5). Thus, alkane eliminations from metastable ions can vary dramatically with the size of the ionic partner in the complex. However, metastable *sec*-butyl ether ions lose only ethane, presumably reflecting the effect of the larger neutral partner (see below).

Competition between R′H elimination and R′ loss above the threshold for the latter may also influence the −R′H/−R′ ratio [3b]. In general, as R increased in size while R′ was kept constant, the portion of the PIE curve for R′H elimination above that for R′ loss decreased, demonstrating diminishing competition of the first process with the second (Figure 2). This

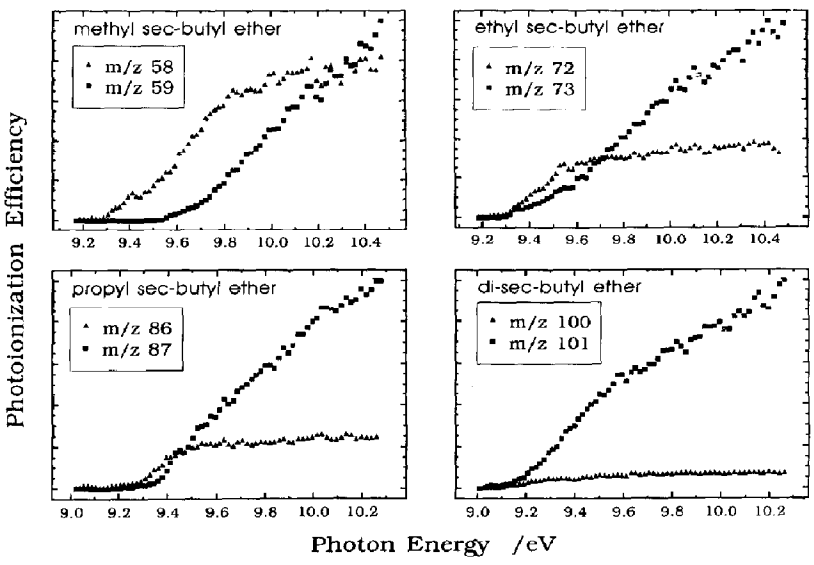

Figure 2. Photoionization ionization efficiency curves for the losses of R′ and R′H from $ROCH(CH_3)R'^{+\cdot}$ ions. These curves demonstrate that as the size of R increases, the competitiveness of R′H elimination with loss of R′ decreases markedly.

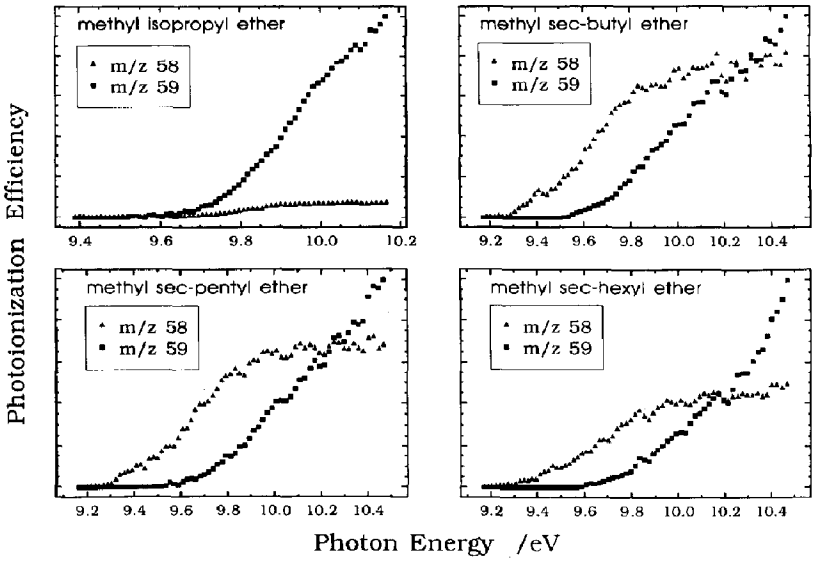

Figure 3. Photoionization ionization efficiency curves demonstrating the effect of increasing the size of R′ on the losses of R′ and R′H from $CH_3OCH(CH_3)R'^{+\cdot}$ ions. These curves indicate that as the size of R′ increases from methyl to ethyl, the competitiveness of R′H elimination with loss of R′ increases markedly.

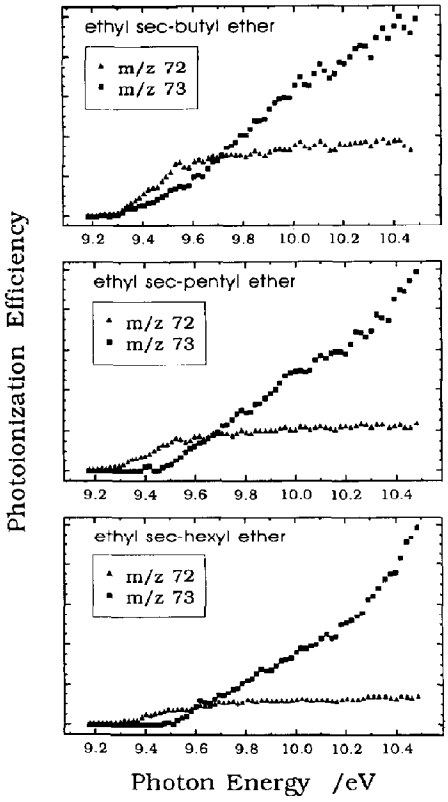

Figure 4. Photoionization ionization efficiency curves for the losses of R′ and R′H from $C_2H_5OCH(CH_3)R'^{+\cdot}$ ions. In contrast to the methyl ethers, as the size of R′ increases, the competitiveness of R′H elimination with loss of R′ seems to decrease.

parallels previous observations on ionized ketones [1]. Competition above the threshold for simple dissociation was assessed in a qualitative way by subtracting $AE(R^+OCHCH_3)$ from the energies at which the PIE curves for loss of R′ and R′H elimination crossed, that is, the photon energies at which the formation of the two species are equal. These crossover energies decreased rapidly as R increased in size (Table 4). Thus, increasing the size of the ion in the complex reduces the direct competitiveness of R′H elimination with R′ loss.

ΔAE decreases dramatically on going from methyl to ethyl *sec*-butyl ether ions, but varies erratically between 5 and 10 kJ mol^{-1} in the larger *sec*-butyl ether ions. Branching in R would weaken the C—C bond cleaved, so the values from ions with such branching may not be comparable to the others.

As $\Delta H_f(CH_3OCH = CH_2^{+\cdot})$ derived from the AE of

Table 2. Differences AE(—R′) − AE(—R′H) and ΔH_f(—R′) − ΔH_f(—R′H)

	$CH_3OCH(CH_3)R'$		$C_2H_5OCH(CH_3)R'$	
Ether	ΔAE^a	$\Delta\Delta H_f^b$	ΔAE^c	$\Delta\Delta H_f^d$
$ROCH(CH_3)_2$	2	26	—	32
$ROCH(CH_3)C_2H_5$	26	8	3	14
$ROCH(CH_3)C_3H_7$	≥ 28[e]	7	22	13
$ROCH(CH_3)C_4H_9$	≥ 33[e]	6	21	12

All values are kJ mol^{-1}.
[a] $AE(CH_3^+OCHCH_3) - AE(CH_3OCH = CH_2^{+\cdot})$.
[b] $\Delta H_f(CH_3^+OCHCH_3) + \Delta H_f(R'^{\cdot}) - [\Delta H_f(CH_3OCH = CH_2^{+\cdot}) + \Delta H_f(R'H)]$ from published values.
[c] $AE(CH_3CH_2^+OCHCH_3) - AE(CH_3CH_2OCH = CH_2^{+\cdot})$.
[d] $\Delta H_f(CH_3CH_2^+OCHCH_3) + \Delta H_f(R'^{\cdot}) - [\Delta H_f(CH_3CH_2OCH = CH_2^{+\cdot}) + \Delta H_f(R'H)]$.
[e] Values are given as ≥ because the lower AE values are maximum values (Table 1). The individual heats of formation from which the $\Delta\Delta H_f$ values are derived are given in the Appendix.

Table 3. CAD spectra of alkane elimination products and of corresponding vinyl ethers

Source	$CH_3OCH=CH_2$[a]	$CH_3OCH(CH_3)C_2H_5$[b]	$C_2H_5OCH=CH_2$[a]	$C_2H_5OCH(CH_3)C_2H_5$[b]	$C_2H_5OCH(CH_3)C_3H_7$[b]	$C_2H_5OCH(CH_3)C_4H_7$[b]
mass-to-charge ratio	58	58	72	72	72	72
15	40	40	2		3	2
26	23	33	3		3	
27	100	95	14	19	15	15
28	72	75	3			
29	80	84	24	40	41	32
30	13	17				
31	78	73	3	4	3	4
41			2		3	5
42	78	81	7	9	10	7
43	87	100	60	67	50	44
44			100	100	100	100
45			12	20	14	19
57	38	44	5	6	7	6

[a]Ions formed in the ion source.
[b]The decompositions of the ionized saturated ethers took place in the first field-free region and CAD spectra were determined in the third field-free region of an electric sector–magnetic sector–electric sector mass spectrometer.

Table 4. Effect of size of R on R'H elimination from $ROCH(CH_3)R'$ ethers

R	$ROCH(CH_3)CH_3$ $-CH_3/-CH_4$[a]	$ROCH(CH_3)C_2H_5$ $-C_2H_5/-C_2H_6$[a]	ΔAE	Crossover[b]
CH_3	< 0.01	< 0.01	26	69
C_2H_5	1.9	0.02	3	38
$CH_3CH_2CH_2$	100	c	7	14
$(CH_3)_2CH$	c	< 0.01	10	3
$CH_3CH_2CH_2CH_2$	> 500	c	c	c
$CH_3CH_2CH(CH_3)$	> 100	< 0.02	5	~ 0

ΔAE and crossover values are kJ mol^{-1}.
[a]Ratios of the heights of peaks representing metastable decompositions.
[b]Photon energy at which the two fragmentations are equal minus $AE(RO^+CHCH_3)$ (see text).
[c]Data not obtained.

that ion formed from *sec*-butyl methyl ether was as low as any obtained, this ion is probably formed close to its thermochemical threshold, that is, the onsets of complex formation and H-transfer between the partners are below the combined heats of formation of the —R'H products. In this situation, the middle traces of Figure 1 represent the potential surface for decomposition. The decrease in ΔAE on going from R = CH_3 to larger alkyl groups suggests that as the ionic partner increases in size, the threshold becomes determined by the onset of bond dissociation rather than product stability. This is the behavior depicted by the bottom traces in Figure 1.

Alkane eliminations were too weak to permit measuring appearance energies for loss of methane from ionized isopropyl ethers larger than the methyl or any of the ionized *tert*-butyl ethers, further evidence that increasing the size of the ion in the complex decreases alkane elimination.

There has been disagreement about whether there is a metastable loss of methyl from ionized isopropyl methyl ether [3a,7]. The resolution of the conflicting reports is that metastable methyl loss from the unlabeled ion is undetectable (present experiments, ref 7), but there is metastable loss of CH_3 when one CD_3 is placed in the *i*-propyl group, as reported in ref 3a.

We attribute the generally decreased competitiveness of R'H elimination with R' loss with increasing size of R to the effect of increasing r predicted by eq 1.

Effect of the size of the neutral partner on alkane elimination. The dependence of R'H elimination on the size of the neutral radical in the intermediate complex was examined by varying R' from CH_3 to $n-C_4H_9$ in methyl and ethyl ether ions. The loss of R'H from metastable ethyl ether ions becomes more important relative to loss of R' as the size of R' increases from CH_3 to C_3H_7 (Table 6). The methyl ether ions lose R'H to the exclusion of R' in metastable decompositions, preventing comparison of —R' and —R'H abundances in that series. The dominance of these alkane losses is attributable to the smaller size of the ionic partner.

ΔAE for the methyl ethers increases as R' became larger, with a large jump between the $^{\cdot}CH_3$ and $^{\cdot}C_2H_5$ partners (Table 2). The products of methane elimination are 26 kJ mol^{-1} more stable than those of methyl loss from ionized isopropyl methyl ether, whereas the corresponding ΔAE = 2kJ mol^{-1}. These results indicate a significant reverse activation energy for this methane elimination. This is confirmed by translational energy releases, ca. 4 kJ mol^{-1} for ionized isopropyl methyl ether versus ca. 1 kJ mol^{-1} for *sec*-butyl methyl ether. (Energy releases were derived from the widths at half maximum height of peaks representing metastable decompositions using the formula $T_{0.5} = V(\Delta m)^2/16m_2m_3$ [11].) The PIE curves (Figure 3) demonstrate that methane loss from ionized isopropyl methyl ether is the least competitive alkane elimination in the methyl ether series, despite its being the most thermochemically favored. We suggest the threshold-determining barrier in this reaction is the one to movement of methyl to the configuration for H-transfer, the situation represented by the bottom traces in Figure 1. The presence of substantial secondary isotope effects [3a] supports a relatively

Table 5. Metastable decompositions of ionized *tert*-butyl ethers

Ether	$-CH_3/-CH_4$
CH_3—O-*tert*-Bu	0.75
C_2H_5—O-*tert*-Bu	50
C_3H_7—O-*tert*-Bu	> 300

CH_3 and CH_4 come from the *tert*-butyl groups (unpublished observations on deuterated *tert*-butyl ether ions).
—CH_4 abundances were too low to permit AE measurements.

Table 6. Effect of size of R' on R'H elimination from $ROCH(CH_3)R'^{+\cdot}$ ions

R'	$CH_3OCH(CH_3)R'$ —R'/—R'H[a]	Crossover	$C_2H_5OCH(CH_3)R'$ —R'/—R'H[a]	Crossover
CH_3	< 0.01	0	1.9	—
C_2H_5	< 0.01	69	0.02	38
C_3H_7	< 0.5	62	< 0.01	18
C_4H_9	< 0.05	55	< 0.01	11

Crossover values are kJ mol^{-1}.
[a]Ratios of the heights of peaks representing metastable decompositions.

high energy for the transition state for bond cleavage relative to that for subsequent H-transfer. Because methyl is very weakly bound, the threshold for methane elimination is close to the energy needed for simple dissociation and substantially above the combined heats of formation of the products of methane elimination. A portion of this excess energy becomes translational energy during decomposition.

For higher members of the methyl ether series, $\Delta AE = 26 - 33$ kJ mol^{-1}, even though $\Delta\Delta H_f$ is only about 6-8 kJ mol^{-1} (Table 2). This reflects a discrepancy between published heats of formation of the vinyl ether ions and the ΔH_fs derived from our $AE(CH_3OCH = CH_2^{+\cdot})$ values (see below). $\Delta H_f(CH_3^+OCHCH_3)$ values derived from the measured AE values are fairly constant and agree well with previous values [3a,12], so the increasing ΔAE values are due to decreasing $AE(CH_3OCH = CH_2^{+\cdot})$ values relative to expected ones. ΔAE does not continue to become larger for the larger methyl ethers because the appearance energies of the alkane eliminations become equal to the ionization energies of the ethers, the lower limit for an AE. This could prevent ΔAE for the losses of C_3H_8 and D_4H_{10} from reflecting the threshold for hydrogen transfer. However, the AEs in question are probably not much too low, as they give the lowest values for $\Delta H_f(CH_3OCH = CH_2^{+\cdot})$, which, as already noted, seem too low. The observation of molecular ions also implies that the measured AEs are not much too low. The larger forces of attraction with increasing size and therefore polarizability of R′ (Table 7) should stabilize ($[RO^+CHCH_3 \cdot R']$) relative to $ROCH = CH_2^+ + R'H$. Therefore, ΔAE could become equal to $\Delta\Delta H_f$ with increasing size of R′ in the methyl ether ions, the situation depicted by the middle traces in Figure 1. The low AE (—R′H) values suggest that this condition is reached in the eliminations of the larger alkanes from ionized *sec*-alkyl methyl ethers.

The crossover energies are fairly constant from 2-butyl to 2-hexyl methyl ether. This suggests that increasing the size of R′ does not make —R′H more competitive than —R′ above the threshold for the latter process.

Ion-induced dipole attractions should increase substantially with each increment in size of the radical in the complex due to corresponding increases in the polarizability of alkyl radicals. This accounts for the large increase in ΔAE on going from $R' = CH_3$ to $R' = C_2H_5$ in the ionized methyl ethers. This change in ΔAE is large because it occurs in the window between $\Delta H_f(CH_3O^+CHCH_3) + \Delta H_f(\cdot R')$ and $\Delta H_f(CH_3OCH = CH_2^{+\cdot}) + \Delta H_f(R'H)$. The 24 kJ mol^{-1} change in ΔAE between $R' = CH_3$ and $R' = C_2H_5$ provides an estimate of the change in the energy needed to form a $[CH_3^+OCHCH_3 \cdot R']$ complex per methylene added in R′, although tunneling [5] may blur this estimate.

ΔAE for the alkane eliminations from the ionized ethyl ethers increases substantially as R′ goes from ethyl to propyl but not from propyl to butyl. In contrast to observations on the methyl ether ions, $AE(C_2H_5OCH = CH_2^{+\cdot})$ remains close to its thermochemical threshold, and $AE(C_2H_5^+OCHCH_3)$ rises with increasing size of R′ in the ionized ethyl ethers. Because $AE(CH_3CH_2OCH = CH_2^{+\cdot})$ formed from ionized *sec*-butyl ethyl ether is at its thermochemical threshold, $AE(ROCH = CH_2^{+\cdot})$ cannot decrease relative to its predicted value with increasing size of R′. The rise in $AE(CH_3CH_2^+OCHCH_3)$ relative to its thermochemical threshold with increasing size of R′ could be attributed to increasing competition from R′H elimination near threshold. However, in contrast to the changes in ΔAE, the crossover energies decrease steadily as the size of R′ increases in the ethyl ether ions (Table 6). This decrease occurs despite the upward shifts in the AE(—R′) values. The small areas between the PIE curves (Figure 4) also do not seem to indicate increasing R′H elimination from the ethyl ethers as R′ increases in size from propyl to butyl. We do not have a clear explanation for this behavior.

ΔH_f of ionized methyl vinyl ether. $\Delta H_f(C_3H_6O^{+\cdot})$ obtained from AE values from the larger methyl ethers are in the range 730–733 kJ mol^{-1} (Table 1), whereas $\Delta H_{f298}(CH_3OCH = CH_2^{+\cdot}) = 754$ kJ mol^{-1} [3a]. This discrepancy indicates errors in the published heats of formation, our measured thresholds, or in the assumed identity of the products. Good agreement between the ΔH_f values for $CH_3^+OCHCH_3$ in Table 1 and the published value suggest that most of the reference heats of formation are accurate. Ab initio calculations (Gaussian 86, HF/6-31G, ZPVE/3-21G [13]) compared with the experimental $\Delta H_f(CH_3COCH_3^{+\cdot})$ give $\Delta H_{f298}(CH_3OCH = CH_2^{+\cdot}) = 755.6$ kJ mol^{-1}. The agreement between theoretical and the published value suggests that the latter is not too high. Its heat of formation (719 kJ mol^{-1}) [12] makes the acetone ion a candidate product of alkane elimination. However, its formation is inconsistent with the CAD spectra and is hard to rationalize on mechanistic grounds. It is also highly unlikely that a more stable product would be formed at threshold in the ion source than upon metastable decomposition. $\Delta H_f(CH_3CH_2OCH = CH_2^{+\cdot})$ from the literature is also higher (10–14 kJ mol^{-1}) than the values derived from our measurements (Table 1).

Table 7. Polarizabilities

CH_4	2.60	CH_3	2.7
C_2H_6	4.44	C_2H_5	4.54
C_3H_8	6.29	n—C_3H_7	6.39
n—C_4H_{10}	8.14	n—C_4H_9	8.24

Values are in Å^3. Values for the alkanes are from ref 16; the value for the methyl radical is from Klots [17], and the values for the remaining radicals are estimated by adding the differences between the corresponding alkane values and the value for methane to the value for methyl.

Summary

Present studies demonstrate that as the size of the ionic partner in an ion-neutral complex increases, H-transfers become less competitive with simple dissociation. This is attributed to decreasing attraction between the partners with increasing distance between the neutral and the center of charge in the ion as the ion increases in size. However, as alkyl radicals in complexes become larger, the onsets for alkane eliminations are lowered relative to those for simple dissociation when product heats of formation permit. This is attributed to a decreasing threshold for alkane elimination relative to that for simple dissociation with increasing polarizability of and therefore stronger attraction to the radical.

Experimental

Decompositions were sampled between the magnetic sector and the second electric sector of a mass spectrometer of the geometry electric sector–magnetic sector–electric sector [14]. All metastable decompositions were determined at an electron impact energy of 70 eV and an ion source temperature of 200 °C. Collisionally activated dissociation spectra were determined by admitting helium to a collision cell to a pressure that gave 20% reduction in the abundance of the primary ion. To obtain CAD spectra of the products of metastable decompositions, the accelerating voltage and magnetic field were adjusted such that the products of first field-free region decompositions passed through the collision cell. Photoionization ionization efficiency curves were determined with a microprocessor-controlled photoionization mass spectrometer as described elsewhere [15]. AE values were obtained by linear extrapolation of the initial rising portion of the curve to the abscissa. Corrections for influences of thermal energy on the curves were made by comparisons to the PIE curves for the corresponding molecular ions. The AE measurements are reproducible to ± 1 kJ mol^{-1}, but the uncertainties due to the contribution of thermal energy can be larger. Heats of formation for fragment ions formed by the process

$$AB + h\nu \rightarrow A^+ + B$$

are related to their AEs by the following formula (assuming no reverse activation energy barriers are present):

$$\Delta H_{f298}(A^+) = AE(A^+) - \Delta H_f(B) + \Delta H_f(AB) + \Delta H_{cor}$$

where ΔH_{cor} is a statistical mechanical correction for thermal energy content that adjusts $\Delta H_f(A^+)$ to 298 K [15a].

Ethers were prepared by standard synthetic methods.

Acknowledgments

We thank the Robert A. Welch Foundation (H-609 to DJM and A1106 to LLG), the Petroleum Research Fund, and the Australian Research Grants Scheme for financial support, Ms. Barbara Kompe for the ab initio calculation of $\Delta H_f(CH_3OCH = CH_2^+)$, Professor Michael Gross and the NSF-supported Midwest Center for Mass Spectrometry for use of the Kratos MS 50TA mass spectrometer, and Ms. Debbie Pavlu for typing.

References

1. Traeger, J. C.; Hudson, C. E.; McAdoo, D. J. *J. Phys. Chem.* **1988**, *92*, 1519.
2. (a) Wendelboe, J. F.; Bowen, R. D.; Williams, D. H. *J. Am. Chem. Soc.* **1981**, *103*, 2333. (b) Tumas, W.; Foster, R. F.; Pellerite, M. J.; Brauman, J. I. *J. Am. Chem. Soc.* **1983**, *105*, 7464. (c) Hudson, C. E.; McAdoo, D. J. *Int. J. Mass Spectrom. Ion Proc.* **1984**, *59*, 325. (d) Hammerum, S. J. *Chem. Soc. Chem. Commun.* **1988**, 858. (e) Bowen, R. D.; Maccoll, A. J. *Chem. Soc. Perkin Trans.* **1990**, *2*, 147.
3. (a) McAdoo, D. J.; Traeger, J. C.; Hudson, C.E.; Griffin, L. L. *J. Phys. Chem.* **1988**, *92*, 1524. (b) Traeger, J. C.; Hudson, C. E.; McAdoo, D. J. *J. Phys. Chem.* **1990**, *94*, 5714.
4. (a) Bowers, M. T.; Jarrold, M. F.; Wagner-Redeker, W.; Kemper, P. R.; Bass, L. M. *Farad. Disc. Chem. Soc.* **1983**, *75*, 57. (b) Redman, E. W.; Morton, T. H. *J. Am. Chem. Soc.* **1986**, *108*, 5701. (c) McAdoo, D. J. *Mass Spectrom. Rev.* **1988**, *7*, 363.
5. Heinrich, N.; Louage, F.; Lifshitz, C.; Schwarz, H. *J. Am. Chem. Soc.* **1988**, *110*, 8183.
6. Hurzeler, H.; Inghram, M. G.; Morrison, J. D. *J. Chem. Phys.* **1958**, *28*, 76.
7. Weiske, T.; Akkok, S.; Schwarz, H. *Int. J. Mass Spectrom. Ion Proc.* **1987**, *76*, 117.
8. Van de Sande, C. C.; McLafferty, F. W. *J. Am. Chem. Soc.* **1975**, *97*, 4617.
9. Hudson, C. E.; Lerner, R. D.; Aleman, R.; McAdoo, D. J. *J. Phys. Chem.* **1980**, *84*, 155.
10. McAdoo, D. J.; Hudson, C. E. *Org. Mass Spectrom.* **1983**, *18*, 466.
11. Cooks, R. G.; Beynon, J. H.; Caprioli, R. M.; Lester, G. R. *Metastable Ions*; Elsevier: Amsterdam, 1973; p 60.
12. Lias, S. G.; Bartmess, J. E.; Liebman, J. F.; Holmes, J. L.; Levin, R. D.; Mallard, W. J. *J. Phys. Chem. Ref. Data* **1988**, *17*, Suppl. 1.
13. Frisch, M. J.; Binkley, J. S.; Schlegel, H. B.; Raghavachari, K.; Melius, C. F.; Martin, R. L.; Stewart, J. J. P.; Bobrowicz, F. W.; Rohlfing, C. M.; Kahn, L. R.; DeFrees, D. J.; Seeger, R. A.; Whiteside, R. A.; Fox, D. J.; Fleuder, E. M.; Pople, J. A. *Gaussian 86*; Carnegie-Mellon Quantum Chemistry Publishing Unit, Pittsburgh, PA, 1984.
14. Gross, M. L.; Chess, E. K.; Lyon, P. A.; Crow, F. W.; Evans, S.; Tudge, H. *Int. J. Mass Spectrom. Ion Phys.* **1982**, *42*, 243.
15. (a) Traeger, J. C.; McLoughlin, R. G. *J. Am. Chem. Soc.* **1981**, *103*, 3647. (b) Traeger, J. C.; McLoughlin, R. G.; Nicholson, A. J. C. *J. Am. Chem. Soc.* **1982**, *104*, 5318. (c) Traeger, J. C. *Org. Mass Spectrom.* **1985**, *20*, 223.
16. Miller, K. J.; Savchik, J. A. *J. Am. Chem. Soc.* **1979**, *101*, 7206.
17. Klots, C. E. *J. Chem. Phys.* **1976**, *64*, 4269.
18. Pedley, J. B.; Rylance, J.; Susex-N. P. L. *Computer Analyzed Thermochemical Data: Organic and Organometallic Compounds*; University of Sussex, England, 1977.
19. (a) Castelhano, A. L.; Griller, D. *J. Am. Chem. Soc.* **1982**, *104*, 3655. (b) Seetula, J. A.; Russell, J. J.; Gutman, D. *J. Am. Chem. Soc.* **1990**, *112*, 1347.

Appendix. Pertinent heats of formation

$CH_3OCH(CH_3)_2$	−252[a]	$CH_3OCH(CH_3)C_2H_5$	−272.6[b]
$CH_3OCH(CH_3)C_3H_7$	−293.2[c]	$CH_3OCH(CH_3)C_4H_9$	−313.8[d]
$C_2H_5OCH(CH_3)_2$	−286.7[e]	$C_2H_5OCH(CH_3)C_2H_5$	−307.3[f]
$C_2H_5OCH(CH_3)C_3H_7$	−327.9[g]	$C_2H_5OCH(CH_3)C_4H_9$	−348.5[h]
$C_3H_7OCH(CH_3)C_2H_5$	−329.1[i]	$(CH_3)_2CHOCH(CH_3)C_2H_5$	−339.8[j]
$[C_2H_5CH(CH_3)]_2O$	−360.4[k]		
$CH_3^+OCHCH_3$	561[l]	$CH_3OCH=CH_2^{+\cdot}$	754[l]
$CH_3CH_2^+OCHCH_3$	521[m]	$CH_3CH_2OCH=CH_2^{+\cdot}$	708[m]
CH_3	144[n]	CH_4	−75[m]
C_2H_5	117[n]	C_2H_6	−84[m]
n—C_3H_7	95[n]	C_3H_8	−105[m]
n—C_4H_9	73[o]	n—C_4H_{10}	−126[m]

[a]Ref 18.
[b]From [a] assuming a group equivalent of −20.6 kJ mol^{-1} for adding CH_2.
[c]From [b] assuming a group equivalent of −20.6 kJ mol^{-1} for adding CH_2.
[d]From [c] assuming a group equivalent of −20.6 kJ mol^{-1} for adding CH_2.
[e]From [a] assuming a group equivalent for replacing CH_3O with C_2H_5O of −34.7 kJ mol^{-1}.
[f]From [b] assuming a group equivalent for replacing CH_3O with C_2H_5O of −34.7 kJ mol^{-1}.
[g]From [e] assuming a group equivalent of 20.6 kJ mol^{-1} for adding CH_2.
[h]From [g] assuming a group equivalent of 20.6 kJ mol^{-1} for adding CH_2.
[i]From [f] assuming −21.8 kJ mol^{-1} for replacing ethoxy with n-propoxy based on ethyl methyl ether = −216.4 kJ mol^{-1} and n-propyl methyl ether = −238.2 kJ mol^{-1} [18].
[j]From di-isopropyl ether = −319.2 kJ mol^{-1} [18] and −20.6 kJ mol^{-1} for adding a CH_2.
[k]From [j] assuming a group equivalent of 20.6 kJ mol^{-1} for adding a CH_2.
[l]Ref 3a.
[m]Ref 12.
[n]Ref 19.
[o]Estimated by extrapolation of the values for the lower members of the series.